

# Energy transport in the presence of long-range interactions

Debarshee Bagchi\*

*Instituto de Física, Universidade Federal do Rio Grande do Sul, Porto Alegre RS, Brazil*

(Dated: March 8, 2021)

We study energy transport in the paradigmatic Hamiltonian mean-field (HMF) model and other related long-range interacting models using molecular dynamics simulations. We show that energy diffusion in the HMF model is subdiffusive in nature, which confirms a recently obtained intriguing result that, despite being globally interacting, this model is a thermal insulator in the thermodynamic limit. Surprisingly, when additional nearest neighbor interactions are introduced to the HMF model, an energy superdiffusion is observed. We show that these results can be consistently explained by studying energy localization due to thermally generated intrinsic localized excitation modes (discrete breathers) in nonlinear discrete systems. Our analysis for the HMF model can also be readily extended to more generic long-range interacting models where the interaction strength decays algebraically with the (shortest) distance between two lattice sites. This reconciles many of the apparently counter-intuitive results presented recently [C. Olivares and C. Anteneodo, *Phys. Rev. E* **94**, 042117 (2016); D. Bagchi, *Phys. Rev. E* **95**, 032102 (2017)] concerning energy transport in two such long-range interacting models.

## I. INTRODUCTION

Long-range (LR) interactions are ubiquitous at all length scales - from cosmology [1] to nanoscience [2] - and are being investigated extensively in recent times. These systems possess extremely rich dynamical and thermodynamical properties that often deviate fantastically from short-range interacting systems. Very frequently these systems exhibit non-ergodicity, weak chaos, inequivalence of ensembles, long-lived non-Gaussian quasistationary states, phase transitions in one dimension, non-concave entropy, and negative specific heat (for reviews see Refs. [3–6]), and as such the conventional thermodynamical formalism of Boltzmann-Gibbs statistical mechanics becomes invalid. These unusual features make the study of LR interacting systems extremely interesting as well as challenging.

Very recently two studies of energy transport in nonlinear one dimensional models with LR interactions have been performed. One of these is for the long-range Fermi-Pasta-Ulam (LR-FPU) model [7] described by the Hamiltonian

$$\mathcal{H} = \sum_{i=1}^N \left[ \frac{p_i^2}{2} + \frac{1}{2}(x_{i+1} - x_i)^2 + \frac{1}{8\tilde{N}} \sum_{j=1}^N \frac{(x_j - x_i)^4}{|i-j|^\delta} \right] \quad (1)$$

and the other is the long-range inertial XY (LR-XY) model [8] (we use the symbol  $\delta$  here instead of  $\alpha$  used in Ref. [8])

$$\mathcal{H} = \sum_{i=1}^N \left[ \frac{p_i^2}{2} + \frac{1}{2\tilde{N}} \sum_{j=1}^N \frac{1 - \cos(\theta_j - \theta_i)}{|i-j|^\delta} \right], \quad (2)$$

where the symbols have their usual meaning. We have set all the coupling constants and mass of each particle

to unity. The factor  $1/\tilde{N}$  in the LR term of both the Hamiltonians ensures extensivity of the potential energy and depends on the parameter  $\delta$ , spatial dimension  $d$  and system size  $N$  [7, 8].

The Hamiltonians of these two models resemble each other in the sense that the nonlinear interaction term in both has been modified in a similar fashion to include LR interactions. Thus each particle interacts with all the other particles in the system and the strength of interaction decays algebraically with the (shortest) distance between the two lattice sites, say  $i$  and  $j$ , as  $|i-j|^{-\delta}$ . The systems described by the Hamiltonians Eqs. (1) and (2) are considered to be long-ranged for  $0 \leq \delta < 1$  and short-ranged if  $\delta > 1$ ; for  $\delta \rightarrow \infty$  we have the nearest-neighbor (NN) interacting models, namely, the Fermi-Pasta-Ulam (FPU) and the inertial XY (coupled rotor) model whereas  $\delta = 0$  corresponds to the mean-field scenario.

In energy transport studies of these two models it was observed that the LR-FPU model exhibits superdiffusive transport for all values of the parameter  $\delta$  [7] whereas the LR-XY model exhibits two distinct phases - an insulator phase for  $\delta < 1$  and a conducting phase  $\delta > 1$  in which Fourier law (implying normal energy diffusion) is obeyed [8]. Moreover, in the LR-FPU, the conductivity  $\kappa$  has an intriguing non-monotonic dependence on  $\delta$  with a maximum conductivity at  $\delta = 2$  whereas the conductivity for the LR-XY model increases monotonically as one increases  $\delta$  from zero.

These results are quite interesting and raise a few questions that need to be addressed. First, why are the transport properties of these two LR systems so strikingly different from each other? In the thermodynamic limit, the LR-FPU is always a thermal conductor (anomalous) with diverging heat conductivity whereas the LR-XY is a thermal insulator for small  $\delta < 1$  and becomes a conductor (normal) obeying Fourier's law for large  $\delta > 1$ .

Second, what is the microscopic mechanism responsible for the existence of an insulator phase in a classical

\* E-mail address:debarshee@cbpf.br

Hamiltonian model where the particles interact via LR interactions? On the contrary, one would expect that, in the presence of global interactions, energy would propagate from one part of the lattice to the other extremely fast. In fact, very recently, an efficient model of a thermal diode was proposed [9] that relied on the idea that LR interactions create additional channels favoring energy flow which may prevent the usual decay of rectification in the thermodynamic limit that typically happens in short-range systems. This idea of increasing the energy flow by LR interactions was previously proposed and analytically investigated, but with an infinitesimal temperature gradient across the system [10]. In another recent work [11] it has been shown that the addition of next-nearest-neighbor interactions is already enough to increase the energy transport and thermal rectification in a mass-graded chain of anharmonic oscillators. In striking contrast, from the study of the LR-XY model it was concluded that the thermal conduction is “spoiled” in the presence of LR interactions [8]. This is the central puzzle that we will investigate here - why the introduction of LR interactions in the FPU model enhances its conductivity significantly whereas doing the same in the XY model, quite surprisingly, turns it into a thermal insulator.

Third, the presence of an insulator phase in the thermodynamic limit demands that the underlying diffusion process should be subdiffusive in nature. This in itself is remarkable since, to the best of our knowledge, apart from one example of a billiard channel model [12], there are no known classical Hamiltonian models that exhibit energy subdiffusion, in the absence of disorder. The well-known one-dimensional Hamiltonian models that have been studied so far exhibit either ballistic transport (seen in integrable models such as the ordered Harmonic lattice), superdiffusive transport (seen in linear momentum conserving systems such as the FPU model), or normal transport (seen in the coupled rotor model and systems with on-site potentials such as the  $\phi^4$  model), but an insulator in the thermodynamic limit is not usually encountered [13, 14]. In fact, as a consequence of the Kac lemma, subdiffusion is argued to be forbidden in conventional Hamiltonian systems due to finiteness of the Poincaré recurrence time [15], although some special cases of subdiffusion have been observed [16].

In this paper, we attempt to obtain a qualitative and, wherever possible, quantitative understanding of the issues raised above. The remainder of the paper is organized as follows. In Sec. II we describe the paradigmatic Hamiltonian mean-field (HMF) model [3-6] which is the mean-field ( $\delta = 0$ ) limit of the LR-XY system described by Eq. (2). We study numerically the HMF model (and some other closely related models) to first show the subdiffusion of energy in Sec. III A, and thereafter in Sec. III B proceed towards extracting a consistent explanation of the thermal transport properties using the concept of intrinsic localized modes of excitation in discrete nonlinear systems. We extend our analysis to the  $\delta > 0$  regime for the LR-XY model in Sec. III C and conclude with a

discussion in Sec. IV.

## II. THE MODEL

The Hamiltonian mean-field model consists of  $N$  particles (or classical planar spins) on a one-dimensional lattice that interact with each other following the energy functional

$$\mathcal{H} = \sum_{i=1}^N \frac{p_i^2}{2} + \frac{1}{2N} \sum_{i,j=1}^N 1 - \cos(\theta_j - \theta_i), \quad (3)$$

where  $p_i$  and  $\theta_i$  are the conjugate momentum and position (on a circle) of the  $i$ th particle. As before, the  $1/N$  factor in the potential energy makes it (and consequently the total energy) extensive, which is the so-called Kac prescription. For the time being we impose periodic boundary conditions. The equation of motion for each particle can be conveniently written in terms of the magnetization components  $M_x = \frac{1}{N} \sum_{i=1}^N \cos \theta_i$  and  $M_y = \frac{1}{N} \sum_{i=1}^N \sin \theta_i$  as

$$\dot{p}_i = F_i = M_y \cos \theta_i - M_x \sin \theta_i, \quad (4)$$

where  $F_i = -\frac{\partial V_i}{\partial \theta_i}$  is the force and  $V_i = \frac{1}{N} \sum_j [1 - \cos(\theta_j - \theta_i)]$  is the potential experienced by the  $i$ -th particle. The share of the total energy that the  $i$ -th particle gets is

$$E_i = \frac{p_i^2}{2} + \frac{1}{2N} \sum_{j=1}^N 1 - \cos(\theta_j - \theta_i). \quad (5)$$

We investigate the properties of this model by numerically integrating the equations of motion using the symplectic velocity Verlet integrator [17] with a small time-step  $\Delta t = 0.01$ . The initial conditions are always assigned randomly from a uniform distribution for the angle variables and from a Gaussian distribution with unit variance for the momenta, both centered around zero. Our results are presented in the next section.

## III. SIMULATION RESULTS

### A. Nature of energy diffusion

First we verify the nature of energy diffusion in the HMF model. Following the equilibrium fluctuation-correlation method, we start from an equilibrated microcanonical system under periodic boundary conditions and monitor how the excess energy at site  $i$  at time  $t_0$  propagates to site  $j$  at a later time  $t_0 + t$ . This is achieved by studying the spatio-temporal correlation of the energy fluctuations which for a microcanonical system (see Refs. [18, 19] for details) is

$$\rho_E(r, t) = \frac{\langle \Delta E_j(t + t_0) \Delta E_i(t_0) \rangle}{\langle \Delta E_i(t_0) \Delta E_i(t_0) \rangle} + \frac{1}{N_b - 1}. \quad (6)$$

As is usually done, we have coarse grained the lattice into  $N_b = N/b$  bins with  $b$  number of particles in each bin and  $r = (i-j)b$ . Here  $\Delta E_k = E_k - \langle E_k \rangle$  is the excess energy of the  $k$ th bin ( $1 \leq k \leq N_b$ );  $E_k$  ( $\langle E_k \rangle$ ) is the instantaneous (average) energy of all the  $b$  particles in the  $k$ th bin calculated using Eq. (5). For our numerical results we set  $b = 4$ . The nature of the energy diffusion process is ascertained from the mean square deviation (MSD) of the function  $\rho_E(r, t)$  denoted as

$$\sigma_E^2(t) = \sum_{r=-N/2}^{N/2} r^2 \rho_E(r, t). \quad (7)$$

For a subdiffusive (superdiffusive) process we should have  $\sigma_E^2(t) \sim t^\beta$  where  $\beta < 1$  ( $\beta > 1$ ) at large times  $t$ ;  $\beta = 1$  corresponds to normal diffusion. After initialization, the momenta are rescaled so that the system has the desired energy density  $u = \langle \mathcal{H} \rangle / N$  and zero net momentum  $\sum_i p_i = 0$ . We evolve this system numerically for a long time  $t = 10^6$  ( $t$  is measured in units of  $\Delta t$  here) until it reaches stationarity. The equilibrated system should have a statistically constant energy profile with  $E_i = u$ . Once this is attained, we start computing the excess energy correlation function  $\rho_E(r, t)$ , and repeat this over several ( $\sim 10^6$ ) initial values of  $t_0$  until well-averaged data are obtained for  $\sigma_E^2(t)$ . We choose a HMF system

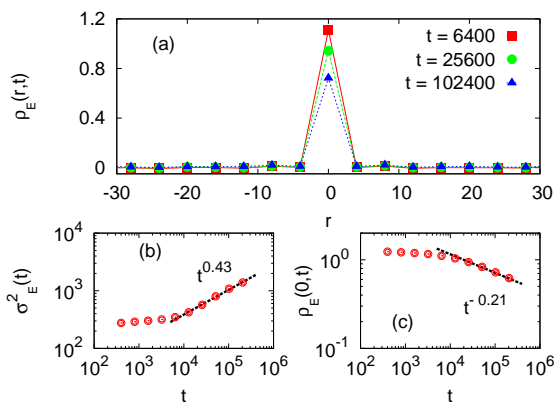


FIG. 1. Subdiffusion of energy in the HMF model for  $N = 200$  and  $u = 1.0$ : (a) the correlation function  $\rho_E(r, t)$  at different times  $t$  (only a small window around  $r = 0$  is shown here), (b) the MSD grows as  $\sigma_E^2(t) \sim t^{0.43}$  and (c) the height decreases with time as  $\rho_E(0, t) \sim t^{-0.21}$  at large times indicating energy subdiffusion.

of size  $N = 200$  which is the largest  $N$  that is studied in Ref. [8] with an energy density  $u = 1.0$ . The correlation function  $\rho_E(r, t)$  at different times is shown in Fig. 1(a). It can be seen that the spread of fluctuations is extremely slow,  $\rho_E(r, t) \approx 0$  for  $r \neq 0$  even for very large  $t > 10^5$ . The MSD  $\sigma_E^2(t)$  is displayed in Fig. 1(b); at large times,  $\sigma_E^2(t) \sim t^{0.43}$ . The height  $\rho_E(0, t)$  of the correlation function decreases with time as  $\rho_E(0, t) \sim t^{-0.21}$ , thus much slower than what one would expect for normal diffusion, i.e.,  $\rho_E(0, t) \sim t^{-1/2}$ . Thus the diffusion process in the

HMF model is indeed subdiffusion with  $\beta < 1$  and the thermally driven system should therefore be an insulator in the thermodynamic limit, as was predicted for a subdiffusive system [13] and numerically demonstrated in Ref. [8]. This is intriguing, as mentioned earlier, that LR interactions enhance thermal transport in the LR-FPU model whereas suppress the same in the LR-XY model.

Next, note that the Hamiltonian for the LR-FPU model also has NN interactions [second term in Eq. (1)], besides the algebraically decaying LR term. In the LR-XY Hamiltonian Eq. (2) a similar NN interaction term is not present. In order to study the effect of additional NN interactions on the nature of energy diffusion, we modify the HMF Hamiltonian as

$$\mathcal{H}_G = \mathcal{H} + \sum_{i=1}^N 1 - \cos(\theta_{i+1} - \theta_i), \quad (8)$$

where  $\mathcal{H}$  is given by Eq. (3). The HMF model with additional NN interactions has been studied earlier [20] and is referred to as the generalized HMF (GHMF) model in the following. The equation of motion now has the form

$$\dot{p}_i = M_y \cos \theta_i - M_x \sin \theta_i + \sin(\theta_{i+1} - \theta_i) + \sin(\theta_{i-1} - \theta_i) \quad (9)$$

To verify if the presence of the NN term leads to a superdiffusive behavior similar to the LR-FPU model we compute, as before, the correlation  $\rho_E(x, t)$  for different times, which is shown in Fig. 2(a) for the same parameters as in Fig. 1. As can be immediately appreciated, the spreading of the correlation function is much faster as compared to the HMF model. At large times the MSD shows  $\sigma_E^2(t) \sim t^{1.5}$  and the height decreases with time as  $\rho_E(0, t) \sim t^{-0.75}$ , as is shown in Figs. 2(b) and 2(c), respectively. Thus a clear superdiffusion is observed at large times with  $\beta > 1$  in this case. This demonstrates

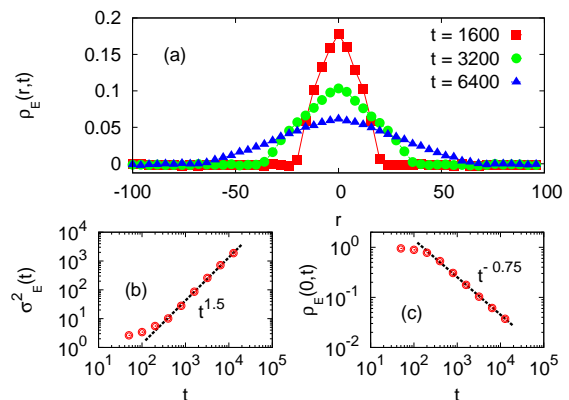


FIG. 2. Superdiffusion of energy in the GHMF model for  $N = 200$  and  $u = 1.0$ : (a) the correlation function  $\rho_E(r, t)$  at different times  $t$ , (b) the MSD grows as  $\sigma_E^2(t) \sim t^{1.5}$  and (c) the height decreases with time as  $\rho_E(0, t) \sim t^{-0.75}$  at large times indicating energy superdiffusion.

that adding a NN interaction term to the HMF model *speeds up* the diffusion process from subdiffusion to superdiffusion. This seems to be counter-intuitive since adding nonlinear interactions usually leads to more scattering of the heat carriers, thus making the transport process slower. As a simple example, adding quartic interactions to the Harmonic oscillator model slows down the diffusion process from ballistic ( $\beta = 2$ ) to superdiffusion ( $1 < \beta < 2$ ) as in the FPU model [21].

We conclude this section by verifying that the nature of energy diffusion for the two models does not change, at least qualitatively, as the system size  $N$  is increased. In Fig. 3(a) the MSD  $\sigma_E^2(t)$  of the HMF model is shown for three different system sizes,  $N = 200, 400$ , and  $800$ . Up to very large times  $t > 10^5$  that we have computed, the  $\sigma_E^2(t)$  for the larger  $N$  is found to have a slower increase with  $t$  as compared to that of a smaller  $N$  value: For  $N = 200, 400$ , and  $800$  we obtain  $\beta \approx 0.43, 0.35$ , and  $0.25$ , respectively. Moreover, the point of inflection for the three curves moves rightwards to larger  $t$  values as  $N$  is increased. Thus a slowdown of energy diffusion happens with increasing  $N$ , which indicates that, in the thermodynamic limit, the energy diffusion will remain subdiffusive for the HMF model. In fact, such a slowing down of the dynamics with increasing system size is well known for this model. It has been observed that relaxation of the HMF model towards the Boltzmann-Gibbs equilibrium becomes exceedingly delayed as  $N$  is increased. This is because the system stays trapped in the so-called *quasi-stationary* states and the relaxation time-scale generally diverges faster than  $N$  [3, 4].

On the other hand, for the GHMF model, the exponent  $\beta$  seems to have negligible finite-size effects, as depicted in Fig. 3(b). The MSD  $\sigma_E^2(t)$  for the three system sizes,  $N = 200, 400$ , and  $800$ , shows identical divergence with an exponent  $\beta \approx 1.5$  at large times. Hence we speculate that the energy diffusion in the GHMF model will remain superdiffusive, even in the thermodynamic limit, akin to the LR-FPU model [7]. In the next section we provide more numerical evidence to justify these results further.

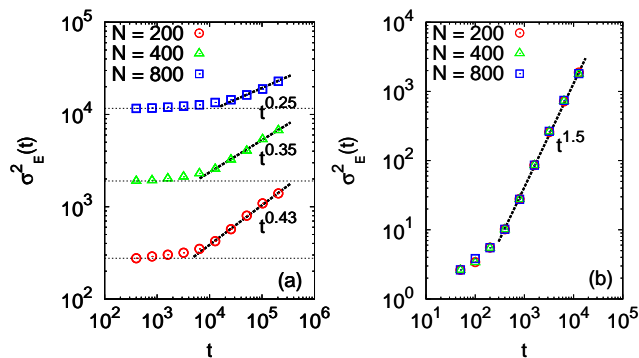


FIG. 3. The MSD  $\sigma_E^2(t)$  as a function of time  $t$  with  $N = 200, 400$ , and  $800$  for (a) the HMF model and (b) the GHMF model. The energy density is fixed at  $u = 1.0$ .

## B. Nonlinear intrinsic localized modes

In order to explain the energy subdiffusion in the HMF model and why additional NN interactions give rise to superdiffusion, we now study certain energy relaxation processes in the HMF (and also the GHMF) model. This is done by performing *boundary cooling* experiments in which one studies how a system relaxes from a high-temperature equilibrium state to a low-temperature equilibrium state in the presence of *absorbing boundaries* [22–24]. In the following, we describe the cooling protocol that has been adopted here.

We begin by immersing our desired model (the HMF or the GHMF with free boundary conditions) in a heat bath at a fixed temperature  $T_b$  which is set to a relatively high value. The stochastic heat bath is modeled by the classical Langevin model [21]. In other words, to *each* particle in the lattice we apply Gaussian white noise and friction (dissipation) at a temperature  $T = T_b$ . The equations of motion become

$$\dot{p}_i = F_i - \gamma p_i + \sqrt{2\gamma k_B T_b} \eta_i, \quad (10)$$

where  $\gamma$  is the friction coefficient and  $\eta_i$  is a delta correlated Gaussian white noise with zero mean (the friction coefficient  $\gamma$  and the Boltzmann constant  $k_B$  are set to unity in all our results). Once the system gets equilibrated under this process at temperature  $T = T_b$ , we remove the system from the heat bath and thereafter apply friction *only* to the two ends of the system. Equivalently, this can be understood as attaching two Langevin heat baths at temperature  $T = 0$  to the end particles at sites  $i = 1$  and  $i = N$ . Explicitly written, the equations of motion now become

$$\dot{p}_i = F_i - \gamma p_i (\delta_{i1} + \delta_{iN}), \quad (11)$$

where  $\delta_{ij}$  is the Kronecker delta function. The system will start to cool off gradually from the equilibrium state at temperature  $T = T_b$  to the equilibrium (ground) state at  $T = 0$  by dissipating heat from the two ends. We allow this boundary cooling to happen for a very long time to allow the system to relax to the ground state.

At this point one might expect that the entire system will relax to the ground state, within a reasonably short time-scale, to have a homogeneous temperature and energy density, consistent with zero temperature. This, however, is not generally true in discrete nonlinear lattices because of the spontaneous thermally generated intrinsic localized modes of excitations often referred to as discrete breathers (DBs) (for recent reviews, see Refs. [25–27]). These are dynamical structures which have been seen in many nonlinear discrete systems, classical and quantum [28], in equilibrium and nonequilibrium, and in any dimension under generic conditions, although their specifics, such as energy thresholds, stability, mobility, etc., may depend on the details of the system in which they appear. These discrete breathers trap a significant fraction of the system’s energy for a long time but



are eventually destroyed in finite systems, thus releasing their trapped energy. In fact, one of the possible explanations for observing normal heat conductivity in the inertial XY model [29] instead of superdiffusive transport, despite being momentum conserving, is attributed to these localized “rotobreathers” preventing the free propagation of phonons regardless of their wavelength or frequency [30, 31]. Thus these cooling experiments are an efficient method of detecting the presence of localized excitation modes and studying their properties.

Here, in the following, we will apply the idea of these intrinsic localized modes to systems with LR interactions. In LR systems, with algebraically decaying interaction strengths, DBs have been studied as mathematical objects [32], but their role in influencing the macroscopic properties, such as relaxation and energy transport, has yet to be investigated. We show that energy localization due to the emergence of these nonlinear excitations can consistently explain all the results discussed above.

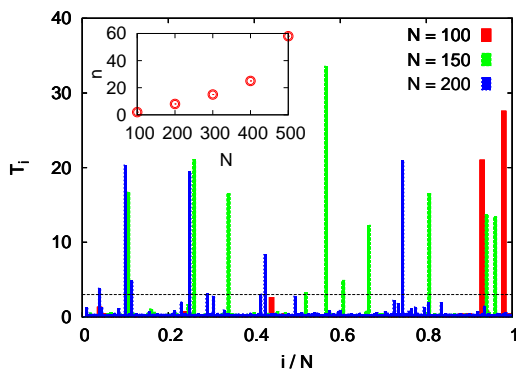


FIG. 4. The temperature profile  $T_i$  of the HMF model for different system sizes  $N = 100, 150$ , and  $200$ . The  $x$ -axis represents the particle indices  $i$  and has been rescaled by the system size  $N$ . The dashed horizontal line indicates the initial temperature  $T_b = 3.0$ . Inset: The number of localized excitations  $n$  having  $T_i > T_b = 3.0$  increases as the system size  $N$  is increased.

Starting from an initial high temperature  $T_b = 3.0$ , we first thermalize the HMF chain. For computational convenience, we intentionally choose a high initial temperature since these intrinsic nonlinear modes are thermally generated excitations and therefore more pronounced at elevated temperatures [22, 23]. After thermalization, we employ the boundary cooling which eliminates most of the delocalized excitations, such as phonons and solitary waves, leaving behind only the localized excitation modes in the system. At this point, we start computing the time-averaged temperature  $T_i = \langle p_i^2 \rangle$  of each particle (or, equivalently, the particle’s energy  $E_i$ ) of the system.

Our result from the boundary cooling experiment is depicted in Fig. 4. We find that, even after allowing an appreciably large time ( $t > 5 \times 10^7$ ) for the system to attain the ground state, there are certain localized regions in the lattice that have temperatures even higher than the initial temperature  $T_b = 3.0$  at which we had equi-

brated our system in the beginning. These “hot spots” trap a large amount of energy and are extremely long-lived, thus indicating that energy diffusion in the lattice is extremely slow or otherwise these localizations would have disappeared because of diffusion of energy from the high-energy to low-energy points in the lattice. This also makes it apparent why the HMF model in the thermodynamic limit behaves as an insulator under thermal bias and exhibits energy subdiffusion. As the system size increases, a large number of these localizations appear and this blocks the passage of energy and renders the lattice non-conducting. Under identical simulation conditions, the number  $n$  of sites with temperature  $T_i > 3.0$  (indicated by the dashed line in Fig. 4) increases with the system size  $N$ , as can be seen in the inset of Fig. 4. Thus, in the thermodynamic limit, the entire lattice essentially splits up into a large number of localized points with negligible interactions among them, which gets reflected also in the result that the correlation  $\rho_E(r, t) \approx 0$  for  $r \neq 0$  that we obtained in the previous section in Fig. 1(a). This also helps us to understand why in Fig. 3(a) the MSD  $\sigma_E^2(t)$  shows a slower increase with time  $t$  (smaller  $\beta$  exponent) when  $N$  is increased.

In Fig. 5(a), we show how the local temperature evolves with time in a HMF lattice of size  $N = 50$  after the boundary cooling is started and the system is allowed to relax to the ground state. We observe that the localizations persist beyond very large times  $t = 10^7$  even in a system of such a small size.

When we perform the same cooling protocol on the GHMF model, we find that the localization effect vanishes at large times. This can be seen by comparing Fig. 5(a) and Fig. 5(b) - the latter appears to be statistically homogeneous at a much shorter time-scales when compared to the former. This shows that, even if energy gets localized initially at some points in the lattice, the presence of the NN interactions makes them unstable. The trapped energy is released and efficiently diffused uniformly in the entire lattice by the LR interactions. This fast annihilation of the energy localizations is negligible in the HMF model because the two-body LR interactions are extremely weak (by a factor of  $N^{-1}$  due to the Kac prescription) as compared to the NN interaction term in the GHMF model. One can clearly see that the diffusion of energy from one site to its neighbors is negligible in the case of the HMF model when compared to the GHMF model.

Now, we compare the results of the HMF and GHMF with the case of the nearest-neighbor XY (rotor) model, which is shown in Fig. 5(c). We perform boundary cooling on the XY model with the same set of parameters and find that energy localization in this case is weaker (having more sites with  $T_i \approx 0$  at large times) as compared to that in the HMF model, but stronger than the GHMF model.

From these results, we can intuitively understand that LR interactions have two competing effects. One is, as we expect, transporting energies over long distances

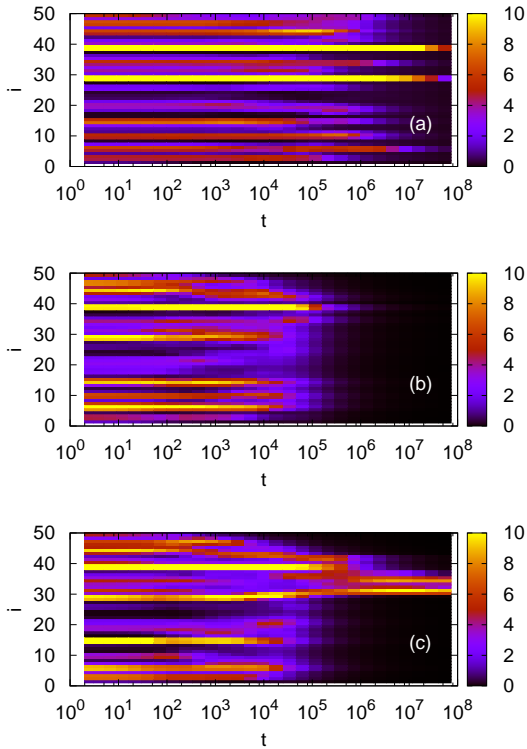


FIG. 5. Variation of the particles' temperature with time  $t$  for (a) the HMF model, (b) the GHMF model, and (c) the inertial XY (coupled rotor) model, all for  $N = 50$ . The  $y$ -axis represents the particle indices on the lattice denoted by  $i$ , and the  $x$ -axis represents time  $t$ . The colors indicate the average temperature  $T_i$  of each particle ranging from  $T_i = 0$  to  $T_i = 10$  as shown in the scale beside each figure.

and thus making energy transport (and equilibration) extremely fast. On the other hand, in the presence of LR interactions energy localization occur abundantly and are extremely long lived. These localized excitation modes impede energy transport in *pure* LR models such as the HMF and exhibit energy subdiffusion. The addition of NN interactions introduces strong local perturbations that cause these localizations to annihilate rapidly. Thus in the presence of both LR and NN interactions, the energy relaxation is the fastest and transport is superdiffusive as in the GHMF model. This justifies why one obtains  $\beta_{HMF} < \beta_{XY} = 1 < \beta_{GHMF}$ , as indicated by our energy diffusion results. These results also make it very clear why introducing LR interactions in the FPU model enhances its thermal conduction whereas it turns the XY model into a thermal insulator.

### C. The $\delta > 0$ regime of the LR-XY model

Until now we have focused mostly on the HMF model which is the  $\delta = 0$  case of the LR-XY model Eq. (2). Let us now extend the idea of localized modes to finite

values of  $\delta > 0$ . In the energy transport study [8] it was found that the conductivity  $\kappa$  monotonically increases with the increase of  $\delta$  from zero (Fig. 2 in Ref. [8]). We speculate that this increase in conductivity with  $\delta$  should get reflected also in the emergence of the localized nonlinear excitation modes. This is what we study in the following.

As before, starting from random initial conditions, we thermalize a LR-XY system with  $N = 500$  particles, by immersing it in a heat bath at temperature  $T_b = 3.0$ . Thereafter we allow it to cool off for a large enough time  $t = 10^6$  using boundary dissipation and compute the local temperature  $T_i$  of the system, from which we will have an estimate of the relative number of localized modes for different values of  $\delta$ . Since the system at large times should ideally have zero temperature at all sites, we set a threshold at a nonzero  $T_{th} > 0$  and identify any site with  $T_i > T_{th}$  as a breather site. The localizations appear for  $\delta > 0$ , as is shown in Fig. 6, but their number  $n$  decreases with increasing  $\delta$ . Under identical simulation conditions, the variation of  $n$  as a function of  $\delta$  is shown in the inset of Fig. 6 with the temperature threshold set at  $T_{th} = 1.0$ . We find that in the LR regime ( $0 \leq \delta < 1$ ) the number of

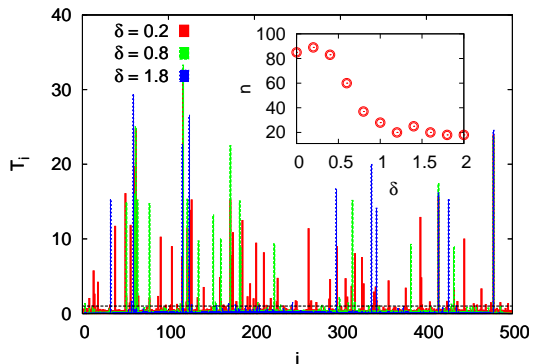


FIG. 6. Temperature profile for the LR-XY model for different values of  $\delta$  with  $N = 500$ . Inset: The number  $n$  is estimated as a function of  $\delta$  with the temperature threshold set at  $T_{th} = 1.0$  represented by the horizontal dashed line in the main figure.

localized excitations  $n$  falls off steadily as the parameter  $\delta$  approaches unity, as shown in the inset of Fig. 6. After crossing the LR regime at  $\delta = 1$ , the number  $n$  seems to be approximately constant. This decrease in  $n$  increases the speed of diffusion as  $\delta$  is increased and one obtains a normal thermal conductor for  $\delta > 1$  from a thermal insulator below  $\delta = 1$ , as was observed in Ref. [8]. Note that the absolute number of localized excitations  $n$  changes as one varies the thermalization time, cooling time, the threshold  $T_{th}$ , initial conditions, size  $N$ , parameters of the system and bath, etc., which is not surprising, but the qualitative feature (the decrease of  $n$  with increase in  $\delta$  from zero) of the result in Fig. 6 remains true nonetheless.

#### IV. DISCUSSIONS

To summarize, we have investigated here the energy transport features of the paradigmatic HMF model and other related LR interacting models. The energy diffusion process in the HMF model is shown to be subdiffusive, whereas an additional NN interaction term leads to superdiffusion, thus re-validating the results obtained in the LR-XY model and the LR-FPU model. We have verified that this result remains true in the LR-FPU model at  $\delta = 0$  as well: If the NN interactions in Eq. (1) are switched off, one obtains an energy subdiffusion akin to the HMF model, thus reinforcing our understanding of the role played by the NN interactions.

Using boundary cooling experiments, we studied the role played by the nonlinear localized modes in influencing energy diffusion and transport in the presence of both NN and LR interactions. We have shown that these modes in the HMF model persist for large times and proliferate as the system size is increased, which ultimately make the model a thermal insulator in the thermodynamic limit. In the presence of additional NN interactions these localized modes annihilate comparatively faster and thus lead to superdiffusive transport as in the GHMF. As the LR parameter  $\delta$  is increased from zero in

the LR-XY model, the number of these localized excitations decreases and this changes the thermal transport from insulating to conducting (obeying Fourier's law) for large  $\delta > 1$ . Note that the boundary cooling experiment does not *generate* the localized excitations but rather *reveals* them by removing the nonlocalized excitations from the system. We believe that a more detailed analysis, taking into account also the mobility of these modes, could be more instructive in understanding thermal transport properties.

Intrinsic localized modes have been observed experimentally in a variety of systems, such as the Josephson junctions, nonlinear optical waveguides, and single crystals [27]. Recently, the HMF Hamiltonian has also been employed to model an experimental system with atoms trapped in an optical cavity [6]. It would be fascinating to observe these localized modes experimentally in a real physical system described by the HMF Hamiltonian.

**Acknowledgments:** The author thanks Y. Levin and R. Pakter for reading the manuscript and an anonymous referee for helpful suggestions. This work is financially supported by CNPq (Brazil).

- 
- [1] T. Padmanabhan, Physics Reports **188**, 285 (1990).
  - [2] French R. H. et al., Rev. Mod. Phys., **82**, 1887 (2010).
  - [3] A. Campa, T. Dauxois, and S. Ruffo, Physics Reports **480**, 57 (2009).
  - [4] F. Bouchet, S. Gupta, and D. Mukamel, Physica A **389**, 4389 (2010).
  - [5] Y. Levin, R. Pakter, F. B. Rizzato, T. N. Teles, and F. P. C. Benetti, Physics Reports **535**, 1 (2014).
  - [6] S. Gupta and S. Ruffo, Int. J. Mod. Phys. A **32**, 1741018 (2017).
  - [7] D. Bagchi, Phys. Rev. E **95**, 032102 (2017).
  - [8] C. Olivares and C. Anteneodo, Phys. Rev. E **94**, 042117 (2016).
  - [9] S. Chen, E. Pereira, and G. Casati, EPL **111**, 30004 (2015).
  - [10] E. Pereira and R. R. Ávila, Phys. Rev. E **88**, 032139 (2013).
  - [11] M. Romero-Bastida, J.-O. Miranda-Peña, and J. M. López, Phys. Rev. E **95**, 032146 (2017).
  - [12] D. Alonso, A. Ruiz, and I. de Vega, Phys. Rev. E **66**, 066131 (2002).
  - [13] B. Li and J. Wang, Phys. Rev. Lett. **91**, 044301 (2003).
  - [14] S. Denisov, J. Klafter, and M. Urbakh, Phys. Rev. Lett. **91**, 194301 (2003).
  - [15] *Microscopic Chaos, Fractals and Transport in Nonequilibrium Statistical Mechanics*, edited by R. Klages, Advanced Series in Nonlinear Dynamics Vol. 24 (World Scientific, Singapore, 2007).
  - [16] G. M. Zaslavsky, Phys. Rep. **371**, 461 (2002).
  - [17] M. P. Allen and D. J. Tildesley, *Computer Simulation of Liquids* (Clarendon, Oxford, U.K., 1989).
  - [18] S. Chen, Y. Zhang, J. Wang, and H. Zhao, Phys. Rev. E **87**, 032153 (2013).
  - [19] Y. Li, S. Liu, N. Li, P. Hänggi, and B. Li, New J. Phys. **17**, 043064 (2015).
  - [20] A. Campa, A. Giansanti, D. Mukamel, and S. Ruffo, Physica A **365**, 120 (2006).
  - [21] A Dhar, Adv. Phys., **57**, 457 (2008).
  - [22] G. P. Tsironis and S. Aubry, Phys. Rev. Lett. **77**, 5225 (1996).
  - [23] G. P. Tsironis, A. R. Bishop, A. V. Savin and A. V. Zolotaryuk, Phys. Rev. E. **60**, 6610 (1999).
  - [24] F. Piazza, S. Lepri, and R. Livi, Chaos **13**, 637 (2003).
  - [25] S. Flach, and C. R. Willis, Phys. Rep. **295**, 181 (1998).
  - [26] S. Aubry, Physica D **216**, 1 (2006).
  - [27] S. Flach, and A. V. Gorbach, Phys. Rep. **467**, 1 (2008).
  - [28] R. S. MacKay, Physica A **288**, 174 (2000).
  - [29] C. Giardinà, R. Livi, A. Politi, and M. Vassalli, Phys. Rev. Lett. **84**, 2144 (2000).
  - [30] O. V. Gendelman and A. V. Savin, Phys. Rev. Lett. **84**, 2381 (2000).
  - [31] O. V. Gendelman and A. V. Savin, Physics of the Solid State, **43**, 355 (2001).
  - [32] S. Flach, Phys. Rev. E **58**, R4116(R) (1998).